J Inorg Organomet Polym (2010) 20:746–754
DOI 10.1007/s10904-010-9409-y

Preparation, Infra-red, MAS-NMR and Structural Characterization of a New Copper Based Inorganic–Organic Hybrid Compound: $[C_5H_6N_2Cl]_2CuCl_4$

Najla Karaa · Besma Hamdi · Abderrazek Oueslati · Abdelhamid Ben Salah · Ridha Zouari

Received: 2 June 2010 / Accepted: 3 September 2010 / Published online: 21 September 2010

Abstract The ionic salt $[2(C_5H_6N_2Cl)^+]$, $[CuCl_4]^{2-}$ complex of copper(II) has been synthesized and characterized. The X-ray diffraction analysis with a single crystal of this compound showed that the title compound (4-amino-2-chloropyridinium)$_2$CuCl$_4$ [(CAP)$_2$CuCl$_4$], crystallized at room temperature in the monoclinic system, space group $C_{2/c}$ (N°.15) and the following : $a = 16.0064$ (2) Å; $b = 7.7964$ (10) Å; $c = 14.7240$ (2) Å; $\beta = 102.497$ (10)°; $V = 1793.91$ (4) Å^3 and $Z = 4$. The structure was solved by using 1,589 independent reflections down to R value of 0.021. The unit cell is made up of tetrachlorocuprate(II) anions and 4-amino-2-chloropyridinium cations linked together by an extensive hydrogen bond network of types N–H···Cl (N: pyridinium) and N–H···Cl (N: amine), and cation-lone pair of nitrogen element interactions. Solid state NMR spectra showed one and five isotropic resonances, ^{63}Cu and ^{13}C, respectively, confirming the solid state structure determined by X-ray diffraction. Impedance spectroscopy study, reported for single crystal, revealed that the conduction in the material was due to a hopping process. This work aims to reveal the thermal properties of a new copper(II) based organic–inorganic hybrid and the conductivity properties that these compounds exhibit.

N. Karaa (✉) · B. Hamdi · A. Ben Salah · R. Zouari
Faculté des Sciences de SFAX, Laboratoire des Sciences des Matériaux et de l'Environnement, PB 1171-3000 Sfax, Tunisie
e-mail: najla_myn@yahoo.fr

A. Oueslati
Faculté des Sciences de SFAX, Unité de l'état Solide, PB 1171-3000 Sfax, Tunisie

Keywords Bis(4-amino-2-chloropyridinium) tetrachlorocuprate(II) · Organic–inorganic hybrid · X-ray diffraction · Infrared spectroscopy · Nuclear magnetic resonance · Thermal analysis · Impedance spectroscopy · Conductivity · Dielectric

1 Introduction

Recently, organic–inorganic hybrid materials have gained great scientific and technological interest due to their interesting properties [1–5] and potential applications, including light emitting diodes, field-effect transistors and solar cells [6–8]. There has been a continuous interest in the chemistry of copper(II) halides due to their stereochemical complexity and the magnetic and optical properties many of them display. The structural chemistry of more than 60 salts containing tetrachlorocuprate(II) ions was summarized a few years ago [9, 10], and many others have been reported more recently [11–23]. The reported copper(II) halides show a wide variety of geometric complexity. Compounds with coordination numbers 4, 5 and 6 with several geometries for each coordination number have been reported. The bridging ability of the halides complicates even more the structural chemistry of these compounds. In addition to the simple mononuclear species, it is possible to obtain oligomeric units ranging from 2 to 14 Cu(II) ions, and infinite one- two- or three-dimensional polymeric species. Willett [24] proposed that it is possible to have some reasonable rationalization for many of these structures through the application of some simple electrostatic arguments which he called 'charged compensation'. According to this idea, the observed structure of copper(II) halides salts can be visualized as a balance between crystal field stabilization effects and an electrostatic ligand–ligand

repulsion effect. In four-coordinate compounds, the former favours a square-planar and the latter a tetrahedral geometry. As long as hydrogen bonds tend to remove charge from the Cl atoms, they will promote the $[CuCl_4]^{2-}$ ion to move toward a square-planar geometry.

In the present investigation, the growth of the crystal of bis(4-amino-2-chloropyridinium) tetrachlorocuprate(II) has been achieved by slow solvent evaporation technique, characterization studies such as single-crystal X-ray diffraction (XRD) studies, solid state nuclear magnetic resonance studies, Fourier transform infrared (FT-IR) spectroscopy, thermal analysis (DSC-TGA) and dielectric studies.

2 Experimental

2.1 Synthesis of $[CAP]_2CuCl_4$ Compound

The first step of material was the preparation of 4-amino-2-chloropyridinium chloride ([CAP] Cl). $[CAP]^+, Cl^-$ crystals were formed by the addition of an aqueous solution of 38% HCl (8 mL) to 4-amino-2-chloropyridine ($C_5H_5N_2Cl$) (2.33 mmol). The dried precipitates were then washed with diethyl ether in order to remove unreacted substances. The next step was the formation of the desired compounds: stoichiometric 2:1 amounts of [CAP]Cl and $CuCl_2$ (1.165 mmol) were dissolved. After several weeks, yellow plate-shaped crystals were obtained by evaporation at room temperature. A single crystal suitable for X-ray diffraction analysis was selected and studied.

2.2 Characterization

Infrared absorption spectroscopy in the 400–4,000 cm^{-1} range; was performed using a Nicole Impact 410 FT-IR spectrometer. The pellets were prepared by mixing 15 mg of powder sample with 300 mg of KBr (The KBr dried at 110 °C) and compressing the whole into a disk. The heating of the $[(CAP)_2CuCl_4]$, pellet in the temperature range 298–425 K; with a heating rate of 10 K min^{-1}, was performed in an air-atmosphere Spectac heating cell. A thermocouple Eurotherm Regler was used for the temperature measurements.

The thermal analyses (TGA) were made on a Perkin Elmer Pyris 6 TGA thermogravimetric analyser. Calorimetric measurements were performed between 298 and 423 K on a Mettler Toledo DSC 822^e calorimeter with a heating rate of 5 K min^{-1} and a sensitivity of 200 μV m W^{-1}.

The NMR experiments were performed at room temperature on a Bruker MSL 300 spectrometer operating at 79.55 MHz for ^{63}Cu and 75.48 MHz for ^{13}C. The powdered sample was packed in a 4 mm diameter rotor and allowed to rotate at speeds up to 10 kHz in a Doty MAS probehead. During the whole acquisition time, the spinning rate of the rotor was locked to the required value thanks to the Bruker pneumatic unit which controls both bearing and drive inlet nitrogen pressures. The spectra were acquired by the use of cross-polarization for proton with 5 ms contact time. All chemical shifts (δ) are given with respect to tetramethylsilane, according to the IUPAC convention, i.e. shielding corresponds to negative values. Spectrum simulation was performed by using Bruker WINFIT software [25]. The chemical synthesis is reproducible, and the formula of the material is determined by structural refinement.

2.3 Crystal Data and Structure Determination

A suitable single crystal of the complex was mounted on a Bruker AXS CCD area detector system for data collection. Unit cell parameters were refined using sets of 830 reflections in the range $2.3 < \theta < 20.3°$.The crystal data of the complex was collected at 292 (2) K. Intensity data were collected in the $\omega - 2\theta$ scan mode using graphite monochromatic Mo K_α radiation (0.71073 Å). The yellow crystal had a flat form with a size of about (0.47 × 0.32 × 0.16) mm^3. The empirical absorption corrections were based on multi-scan. The structure was solved using the Patterson method with the SHELXS 86 program [26]. The refinement was done by full-matrix least squares methods (SHELXL 97 program) [27] and converged to an acceptable final agreement factor. The hydrogen atoms were refined isotropically. The crystal data and details of data collection and refinement for $[CAP]_2CuCl_4$ are summarized in Table 1. The atomic coordinates and equivalent isotropic and anisotropic thermal agitation factors are listed in Tables 2 and 3, respectively. The structural graphics were created with ORTEP [28] (Fig. 1) and DIAMOND [29] (Fig. 2).

2.4 Electrical Measurements

The electrical measurements were performed using a two-electrode configuration on polycrystalline samples. The polycrystalline sample was pressed into pellets of 8 mm diameter and 0.9 mm thickness. Electrical impedances were measured in a frequency ranging from 209 Hz to 5 MHz with the TEGAM 3550 ALF automatic bridge monitored by a microcomputer between 391 and 423 K.

3 Results and Discussion

3.1 X-ray Diffraction

The asymmetrical unit of the bis(4-amino-2-chloropyridinium) tetrachlorocuprate(II) consists of one crystallographically independent CAP organic cation and a half isolate $[CuCl_4]^{2-}$ anion as shown in Fig. 1.

Table 1 Summary of crystal data, intensity measurements and refined parameters of $[CAP]_2CuCl_4$ compound

Crystal data	
Empirical formula	$[C_5H_6N_2Cl]_2CuCl_4$
Formula weight	464.49
Crystal system	Monoclinic
Space group:	*C*2/*c*
Hall symbol:	−C 2yc
Unit cell dimensions	
a (Å)	16.0064 (2)
b (Å)	7.7964 (10)
c (Å)	14.7240 (2)
β (°)	102.497 (10)
Volume (Å^3)	1793.91 (4)
Z	4
D_{calc} (mg m^{-3})	1.720
Absorption coefficient (mm^{-1})	2.11
F(000)	924
Crystal dimensions (mm)	0.47 × 0.32 × 0.16
Crystal color	Plate, yellow
θ Range for data collection (°)	2.3–20.3
Data collection	
Reflections collected	15357
Independent reflections	1589 [$R_{int} = 0.019$]
Reflections with $I > 2\sigma(I)$	1480
Limiting indices	$h = -18 \rightarrow 18$
	$k = -9 \rightarrow 9$
	$l = -17 \rightarrow 17$
CCD area detector diffractometer radiation source: fine-focus sealed tube graphite *φ* and *ω* scans absorption correction: multi-scan North et al. (1968)	$T_{min} = 0.445$, $T_{max} = 0.72$ $\theta_{max} = 25.0°$, $\theta_{min} = 2.6°$
Refinement	
Refinement method	Full-matrix least-squares on F^2
$R[F^2 > 2\sigma(F^2)]$	0.021
$wR(F^2)$	0.054
Goodness-of-fit on F^2	$S = 1.07$
Data/restraints/parameters	1589/0/97
Extinction coefficient	0.0017 (2)
$\Delta\rho_{max}$ (e Å^{-3})	0.47
$\Delta\rho_{min}$ (e Å^{-3})	−0.31

Primary atom site location: structure-invariant direct methods

Secondary atom site location: difference Fourier map

Hydrogen site location: inferred from neighbouring sites

H-atom parameters constrained

$w = 1/[\sigma^2(F_o^2) + (0.0234P)^2 + 1.7937P]$ where $P = (F_o^2 + 2F_c^2)/3$

$(\Delta/\sigma)_{max} < 0.001$ extinction correction: SHELXL

The $[CuCl_4]^{2-}$ anion is a flattened tetrahedron, with two bond angles distinguishing their high values [136.11 (2)°] from the rest [96.61 (2), 99.34 (2)°]. The bond distances Cu–Cl range from 2.2270 (6) to 2.2566 (6) Å with an average <Cu–Cl> of 2.2418 Å. A full list of bond lengths and angles is given in Table 4. The shorter Cu–Cl distance is the Cl(2) atom not involved in (pyridine) N(2)–H···Cl hydrogen bonding. This arrangement seems to be quite common for organo-halocuprates(II) in which the isolated $[CuCl_4]^{2-}$ anions form strong hydrogen contacts of type N–H···Cl (N-pyridine) with the organic cations [24, 30]. High values of the Cl–Cu–Cl bond angles (above 130°) and substantial distortions of the tetrahedral symmetry towards a square-plane one are found as the hydrogen-bonding capabilities of the cations increase. The $[CuCl_4]^{2-}$ anions are placed between these cations layers and establish N–H….Cl hydrogen bonds (N: pyridine and N: amine) contacts along the [110] direction (Fig. 2). The main interatomic distances and angles involved in hydrogen bonds are listed in Table 5.

The geometry of the cation is normal, and its packing appears to be largely dictated by hydrogen-bonding constraints. Figure 2 shows a view of the complex crystal structure, together with the network of hydrogen contacts (dotted lines). The planar organic cations form parallel columns stacked along the *a* and *b* axis. The cations are tilted with respect to the *ab* plane and the centre of symmetry. Cation (I) and cation (II) (Fig. 3) are almost parallel to each other and are titled with respect to the *bc* and *ac* planes. The interstacking distances of *bc* and *ac* are equal to 3.51 Å which is comparable to interplanar distances found in the aromatic *π*-system and lone pair of nitrogen element (3.4–3.6 Å) with strong interactions [31].

3.2 FT-IR Spectra

The IR absorption frequencies of the title complex bis(4-amino-2-chloropyridinium) tetrachlorocuprate(II), $[CAP]_2CuCl_4$, are compared with those of free 4-amino-2-chloropyridine and 4-amino-2-chloropyridinium chloride. The attribution of vibrational modes is consistent with that reported in the literature [32, 33]. Figure 4 shows the FT-IR spectra of the three compounds at room temperature. A detailed assignment of all the bands is difficult, but we can attribute some of them by comparison with similar compounds [34–36].

The principal bands are assigned to the internal modes of the three compounds. The C=C bands exhibit torsion vibration at almost 440 cm^{-1} and stretching vibration at the 1,900–2,000 cm^{-1} range. The bands observed at 995 cm^{-1} are ascribed to the CH wagging mode. Those observed at 1,136 and 1,330 cm^{-1} are ascribed to CH bending vibration. The CH stretching vibrations are observed in the 3,020–3,100 cm^{-1} range. The bands observed at 788 cm^{-1} are associated to the C–Cl and those at 1,570 cm^{-1} to NH_2. The FT-IR spectra of the title

Table 2 Details of atomic and equivalent thermal factors of agitation U_{eq} (Å^2) and isotropic U_{iso} (Å^2) * in $[CAP]_2CuCl_4$ compound

	X	Y	Z	U_{iso}*/U_{eq}
C1	0.213 (13)	0.468 (3)	−0.008 (13)	0.044 (6)
C2	0.136 (13)	0.394 (3)	−0.043 (13)	0.047 (6)
C3	0.085 (12)	0.341 (3)	0.017 (13)	0.046 (6)
C4	0.115 (13)	0.372 (3)	0.112 (14)	0.049 (6)
C5	0.192 (13)	0.446 (3)	0.142 (14)	0.051 (7)
N1	0.010 (11)	0.265 (3)	−0.013 (14)	0.064 (7)
N2	0.241 (11)	0.493 (2)	0.082 (12)	0.048 (5)
Cl	0.280 (4)	0.535 (8)	−0.077 (4)	0.063 (2)
Cu	0.000	0.003 (4)	0.250	0.039 (1)
Cl1	0.087 (3)	0.195 (7)	0.162 (4)	0.054 (2)
Cl2	0.099 (3)	−0.181 (7)	0.227 (3)	0.054 (2)
H2	0.118	0.377	−0.107	0.056*
H4	0.082	0.340	0.155	0.059*
H5	0.212	0.466	0.206	0.062*
H1A	−0.008	0.248	−0.072	0.077*
H1B	−0.020	0.234	0.025	0.077*
H2A	0.290	0.540	0.103	0.057*

complex and 4-amino-2-chloropyridinium chloride show the strongest peak at 3,300 cm^{-1} due to the asymmetric/symmetric N–H stretching vibration of the pyridinium $(N–H)^+$. A series of overtone peaks ranging from 2,400 to 2,900 cm^{-1} are also observed due to N–H stretching. Great changes occur in the FT-IR spectra of $[CAP]_2CuCl_4$; this can be attributed to the chemical environment change of (N–H) pyridine groups. This indicates that N–H….Cl hydrogen bands are formed in the hybrid, with an intensity weaker than that of 4-amino-2-chlorohydrpyridinium chloride. In the hybrid crystal, Van der Waals interactions between the organic chains and Coulomb forces between the positively charged organic and the negatively charged inorganic sheets account for the weak hydrogen bonding.

An infrared spectroscopic study in the temperature range 298–425 K was undertaken in order to gain more information on the crystal dynamics of the $[CAP]_2CuCl_4$ sample. The IR study was restricted to the frequency range 3,000–4,000 cm^{-1}, where exist the intensity of the band characteristic of water molecules; is at about 3,550 cm^{-1}.

IR spectra are presented in Fig. 5 (above T = 358 K all the spectra are superposed). From these curves, it could be seen that up to about 308 K, the intensities of the characteristic bands of water molecules decrease gradually and vanish totally at about 358 K.

These spectroscopic results show that the title compounds lose water molecules gradually from 308 to 358 K.

3.3 Thermal Property

DSC measurements and TGA analysis were carried out to characterize the thermal stability of the complex $[CAP]_2CuCl_4$, which are shown in Fig. 6. The melting–decomposition transition (from DSC) and weight loss process (from TGA) were studied. The curves show that the water molecule starts rather abruptly at approximately 310 K and continues up to approximately 370 K (obs. loss. = 0.38 ± 0.1%). For water molecules, the temperature 310 K is too low to be evaporated instantly. An endothermic transition which occurred at 423 K corresponds to the melting process, followed by an obvious endothermic transition assigned to the melting of the $[CAP]_2CuCl_4$ complex.

3.4 RMN Spectroscopy

The ^{63}Cu MAS-NMR spectrum of the compound is shown in Fig. 7. The spectrum is composed of one broad peak. The δ_{iso} value is equal to 2,325.57 ppm indicating that $CuCl_4^{2-}$ tetrahedral is present in the sample.

The ^{13}C MAS-NMR of the crystalline bis(4-amino-2-chloropyridinium) tetrachlorocuprate(II), permits to

Table 3 Factors of anisotropic thermal agitation of $[CAP]_2CuCl_4$ compound

	U11	U22	U33	U12	U13	U23
C1	0.0460 (10)	0.0444 (10)	0.0421 (10)	0.0115 (8)	0.0087 (8)	0.0040 (8)
C2	0.0527 (11)	0.0498 (11)	0.0344 (9)	0.0083 (9)	−0.0003 (8)	−0.0027 (8)
C3	0.0459 (11)	0.0443 (10)	0.0442 (10)	0.0039 (8)	−0.0003 (8)	−0.0023 (8)
C4	0.0495 (11)	0.0595 (12)	0.0396 (10)	−0.0003 (10)	0.0075 (8)	−0.0003 (9)
C5	0.0512 (12)	0.0650 (13)	0.0356 (10)	0.0015 (10)	0.0010 (9)	−0.0056 (9)
N1	0.0549 (11)	0.0802 (14)	0.0536 (11)	0.0152 (10)	−0.0006 (8)	−0.0089 (10)
N2	0.0396 (9)	0.0561 (10)	0.0455 (9)	−0.0021 (7)	0.0022 (7)	−0.0037 (7)
Cl	0.0587 (3)	0.0761 (4)	0.0588 (3)	0.0100 (3)	0.0220 (3)	0.0125 (3)
Cu	0.0338 (2)	0.0445 (2)	0.0385 (2)	0.0000	0.0039 (1)	0.0000
Cl1	0.0389 (3)	0.0559 (3)	0.0623 (3)	0.0003 (2)	−0.0047 (2)	0.0131 (2)
Cl2	0.0498 (3)	0.0657 (3)	0.0476 (3)	0.0146 (2)	0.0082 (2)	−0.0069 (2)

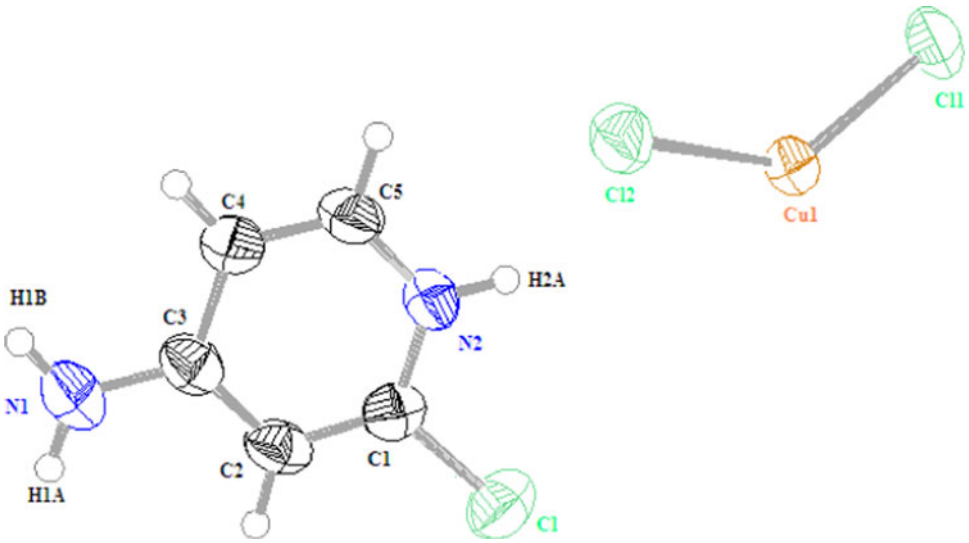

Fig. 1 The asymmetric unit in the $[CAP]_2CuCl_4$ compound. Ellipsoid represented at 50% probability level; only hydrogen atoms for nitrogen are labeled

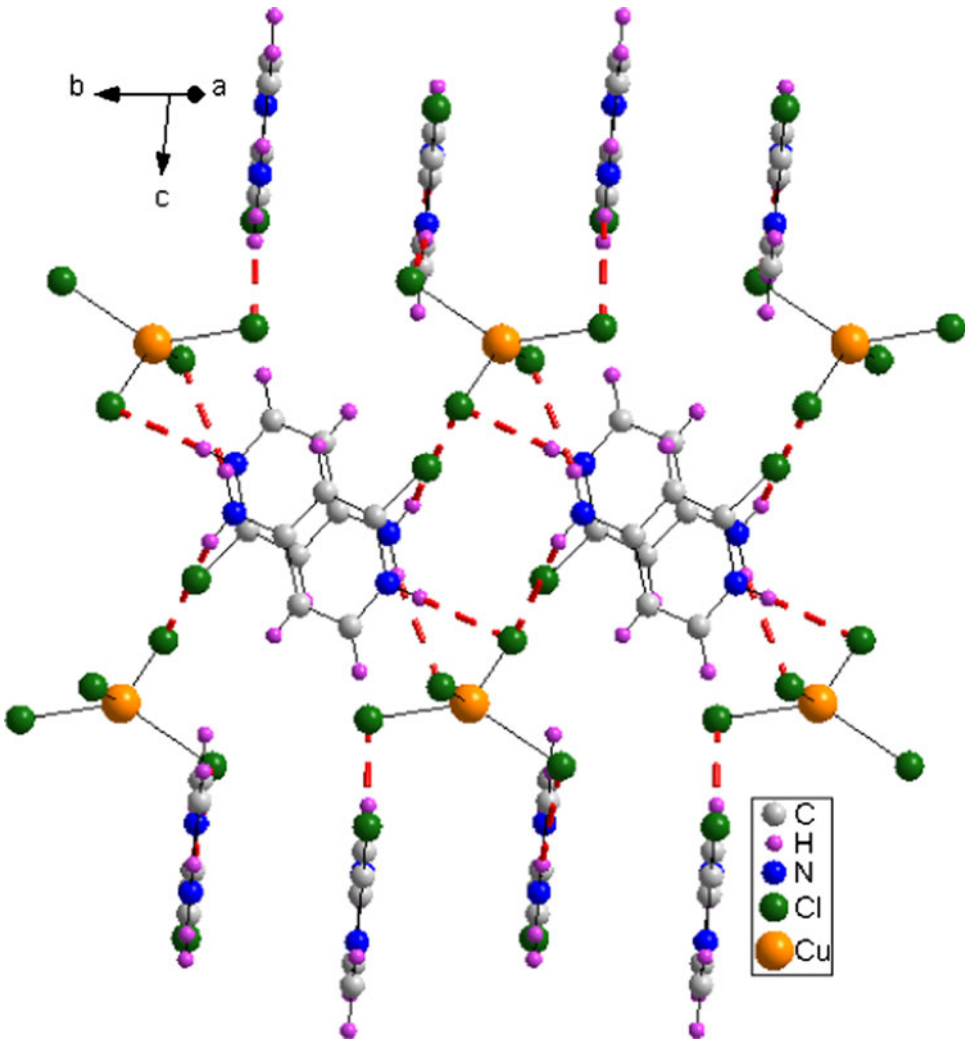

Fig. 2 Packing diagram showing the two orientations of the cations in $[CAP]_2CuCl_4$. *Dotted lines* represent hydrogen bonds

identify five peaks (Fig. 8; Table 4) corresponding to the five carbon atoms of the organic cation; this result proves the presence of only one organic cation in the asymmetric unit of the compound in agreement with the X-ray diffraction data. The chemical shift to a higher frequency can be explained by the fact that the two carbon atoms C(1) and

Table 4 Main distances (Å) and bond angles (°) in the cationic and anionic parts of the $[CAP]_2CuCl_4$ compound

Distances (Å)		Angles (°)	
$[CuCl_4]^{2-}$			
Cu–Cl1	2.2566 (6)	Cl1–Cu–Cl1i	96.61 (2)
Cu–Cl1i	2.2566 (6)	Cl1–Cu–Cl2i	98.06 (2)
Cu–Cl2	2.2270 (6)	Cl1i–Cu–Cl2	98.06 (2)
Cu–Cl2i	2.2270 (6)	Cl2–Cu–Cl2i	99.34 (2)
		Cl1–Cu–Cl2	136.11 (2)
		Cl1i–Cu–Cl2i	136.11 (2)
$[C_5H_6N_2Cl]^+$			
N1–C3	1.329 (3)	Cl–C1–N2	115.68 (16)
N2–C1	1.340 (3)	C2–C3–C4	117.75 (19)
C1–C2	1.346 (3)	C1–C2–C3	119.36 (18)
N2–C5	1.347 (3)	C3–C4–C5	119.63 (19)
C4–C5	1.349 (3)	C1–N2–C5	120.28 (18)
C2–C3	1.403 (3)	N1–C3–C4	120.47 (19)
C3–C4	1.408 (3)	N2–C5–C4	121.12 (19)
Cl–C1	1.714 (2)	N1–C3–C2	121.79 (18)
		N2–C1–C2	121.85 (19)
		Cl–C1–C2	122.47 (15)
Torsion angles			
C5–N2–C1–Cl	179.37 (16)	C1–C2–C3–N1	−179.1 (2)
C5–N2–C1–C2	−0.4 (3)	C1–C2–C3–C4	1.1 (3)
C1–N2–C5–C4	0.4 (3)	N1–C3–C4–C5	179.1 (2)
Cl–C1–C2–C3	179.84 (18)	C2–C3–C4–C5	−1.1 (3)
N2–C1–C2–C3	−0.4 (3)	C3–C4–C5–N2	0.4 (3)

Symmetry codes: (i) $-x, y, -z + 1/2$; (ii) $-x, -y, -z$; (iii) $x, -y, z + 1/2$; (iv) $x - 1/2, y - 1/2, z$; (v) $-x + 1/2, y - 1/2, -z + 1/2$; (vi) $-x + 1/2, -y + 1/2, -z$; (vii) $-x, -y + 1, -z$; (viii) $x, y - 1, z$; (ix) $x, -y + 1, z - 1/2$; (x) $x + 1/2, y + 1/2, z$; (xi) $x, y + 1, z$; (xii) $-x + 1/2, y + 1/2, -z + 1/2$; (xiii) $x, -y, z - 1/2$; (xiv) $x, -y + 1, z + 1/2$

Table 5 Main inter-atomic distances (Å) and bond angles (°) involved in the hydrogen bonds of $[CAP]_2CuCl_4$ compound

D–H···A	D–H	H···A	D···A	D–H···A
N1–H1A···Cl2^{ii}	0.8600	2.4900	3.323 (2)	164.00
N1–H1B···Cl1	0.8600	2.5100	3.347 (2)	166.00
N2–H2A···Cl1^{x}	0.8600	2.3100	3.1615 (18)	173.00

Symmetry codes: (ii) −x, −y, −z; (x) $x + 1/2, y + 1/2, z$

C(5) of the aromatic-ring, are linked to the N(1) pyridinic atoms [37, 38].

3.5 Electric Properties

Figure 9 shows the complex impedance measurements of the $[CAP]_2CuCl_4$ sample at various temperatures. Typical semicircles are obtained. As the temperature increases to 318 K, the semicircles move to a lower value of impedance. These semicircles move to a heat value of impedance when the temperature increases to 358 K and they return to a lower value of impedance. The variation of the semicircles is explained by a partial weight loss associated to the evaporation of the water molecules, which is the result of the DSC and TGA curves of the simple.

To better understand the structure, the impedance analyses were conducted to separate the possible contributions of grains, grain boundaries and electric-electrode interface effect. A schematic model of the sample was described by the equivalent circuit (Fig. 10), which was proposed in the literature [39, 40]. The circuit consists of a series connection of three sub-circuits, one represents grains, the other represents the grain boundary phase and the third the electric-electrode interface. Each sub-circuit is composed of one resistor and capacitor in parallel. The impedance of such an equivalent circuit can be described by both the real part, Z', and the imaginary part, Z'' as follows [40]:

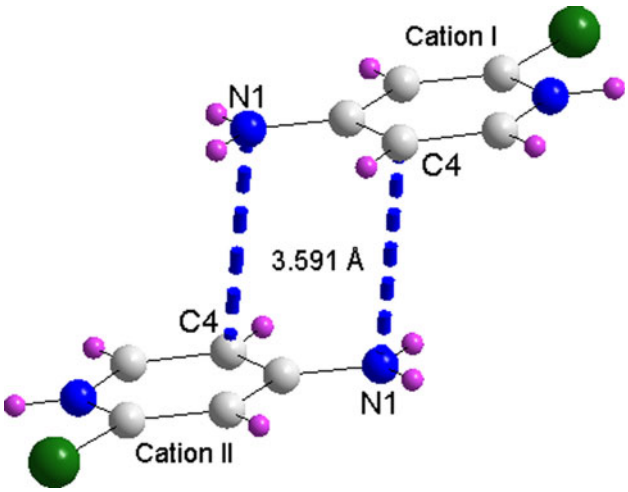

Fig. 3 The π-lone pair of nitrogen interactions between the chains of aromatic ring

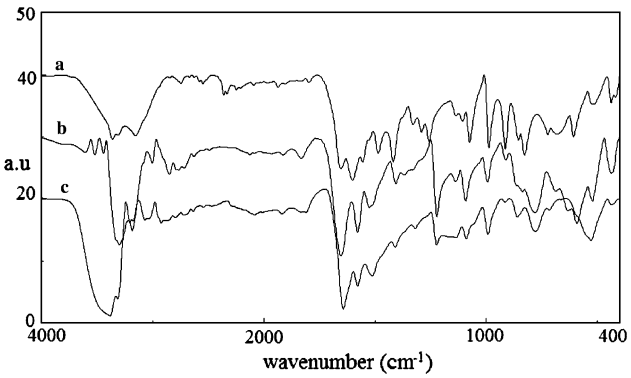

Fig. 4 FT-IR spectra of (*a*) $C_5H_5N_2Cl$, (*b*) $[C_5H_6N_2Cl]Cl$ and (*c*) $[C_5H_6N_2Cl]_2CuCl_4$ at room temperature

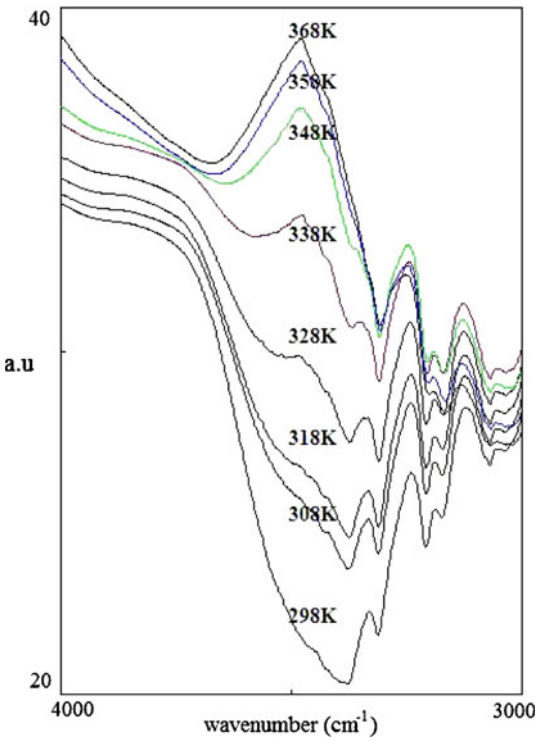

Fig. 5 IR spectra at different temperatures of $[CAP]_2CuCl_4$ compound

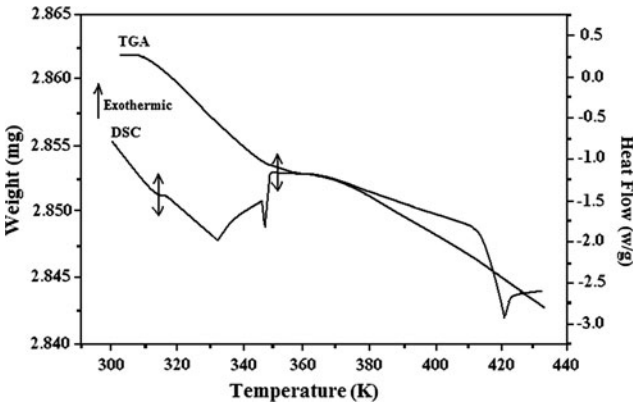

Fig. 6 The simultaneous DSC and TGA curves of $[CAP]_2CuCl_4$ compound

$$\underset{(RHC)_k}{Z(w)} = \sum_k \frac{R_k}{(1+R_k^2\,C_k^2\,w^2)} - j\sum_k \left|\frac{R_k^2\,Cw}{(1+R_k^2\,C_k^2\,w^2)}\right|$$

$$= Z' - jZ''$$

$$w_0^k = \frac{1}{R_k\,C_K}$$

Where $\omega = 2\pi f$ is the angular frequency, C_k and R_k are the capacitance and resistance of grains, grain boundaries and electric-electrode interface (C_{Hf}, R_{Hf}, C_{Mf}, R_{Mf}, C_{Lf} and R_{Lf}), respectively. A typical $Z'' - Z'$ plot with fitting curves of the sample at T = 423 K is represented in

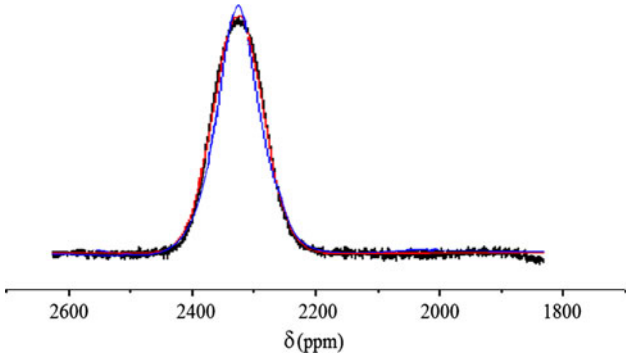

Fig. 7 Plots of experimental and fitted curves of the isotropic band of the ^{63}Cu MAS-NMR spectrum of $[CAP]_2CuCl_4$ compound

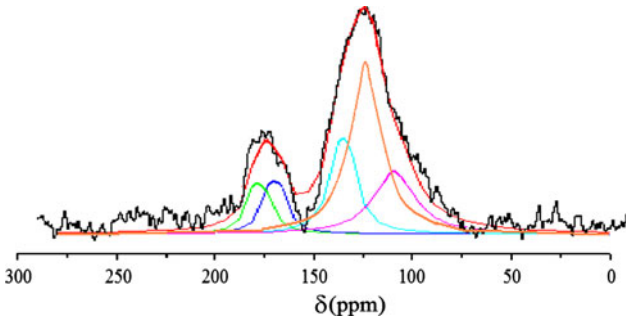

Fig. 8 Plots of experimental and fitted curves of the isotropic band of the ^{13}C MAS-NMR spectrum of $[CAP]_2CuCl_4$ compound

Fig. 10. There are mainly three overlapping semicircles, which correspond to grains (the semicircle on the left-hand side), grains boundaries (the semicircle in the middle) and the electric-electrode interface (the semicircle on the right-hand side).

The $Z'' - Z'$ plots were predominated by twin semicircles with a little deviation at the low frequency range. The predominant semicircle represents the grain, whereas the grain boundaries and the electric-electrode interfaces have a less significant contribution to the impedance.

The Arrhenius plots of the measured electrical conductivity σ of the grain, grain boundary and electric-electrode interfaces as a function of reciprocal temperature of $[CAP]_2CuCl_4$ sample are shown in Fig. 11. The change of conductivity with absolute temperature shows three regions separated by two temperatures, $T_1 = 328$ K and $T_2 = 358$ K. The middle region is associated to the evaporation of the water molecules (region III).

The activation energies are obtained from the slopes of the two straight line segments using the well-known relationship [41–43]:

$$\sigma T = \sigma_0 e^{\left(-\frac{\Delta E}{K_\beta T}\right)}$$

where σ is the conductivity at temperature T, σ_0 the pre-exponential factor, K_β the Boltzmann's constant and

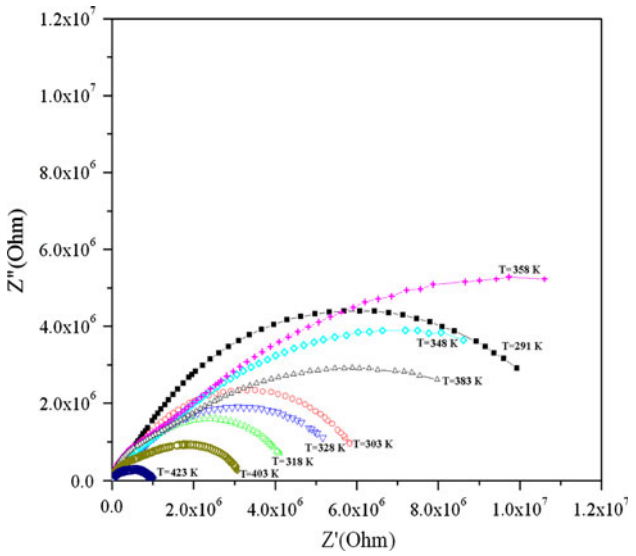

Fig. 9 Impedance spectra of $[CAP]_2CuCl_4$ sample at different temperature ranges

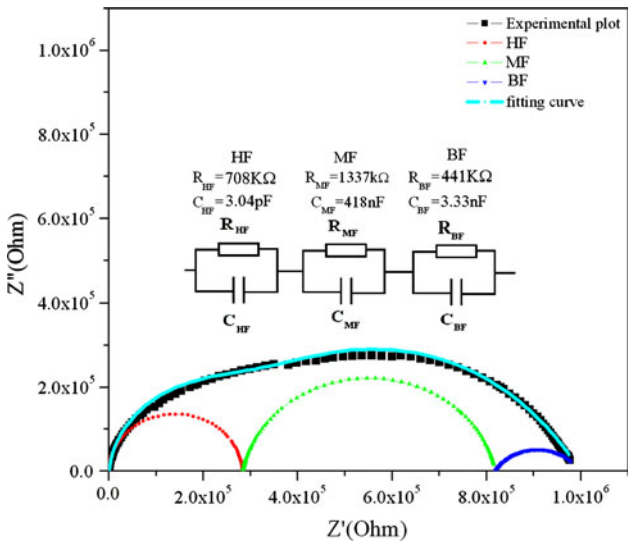

Fig. 10 Complex impedance plane plots at 423 K and equivalent circuit mode of $[CAP]_2CuCl_4$ compound

ΔE the thermal activation energy for the ion migration (Table 6).

The activation energies which correspond to the total measurement (before fitting), grains, grains boundaries and electric-electrode interface (obtained after fitting) are summarized in Table 7. The activation energies of sample, in the two regions, correspond to the total measurement, predominated by the activation energies of grains boundaries and electric-electrode interface.

However, the values of the activation energies of conduction, especially for the grain part, are equal to 0.08 and 0.44 eV, which are reasonably in agreement with the data reported in the literature [44]. Thus, it is likely that the

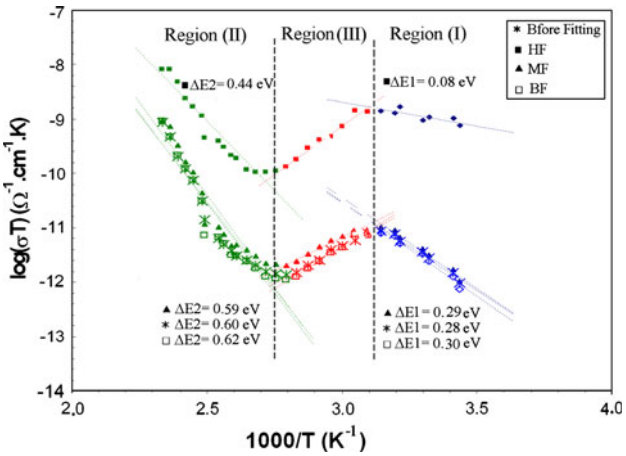

Fig. 11 Arrhenius plots of conductivity of $[CAP]_2CuCl_4$ compound

Table 6 The chemical shifts of carbons in ^{13}C NMR spectra of $[CAP]_2CuCl_4$ compound

Peaks	δ_{iso} (ppm)	FWHM (ppm)
C1	179.34	6.14
C2	109.51	13.74
C3	139.15	12.73
C4	124.15	16.47
C5	169.72	9.40

Table 7 Energy activation (eV) before and after fitting of $[CAP]_2CuCl_4$ compound

	Before fitting	BF	MF	HF
ΔE_1 (region I)	0.28	0.30	0.29	0.08
ΔE_2 (region II)	0.60	0.62	0.59	0.44

observed change is due to a change in the conduction mechanism because the calorimetric study shows one single endothermic peak, in the temperature range 328–358 K, assigned to the evaporation of the water molecules. The activation energy increases with increasing temperature. The activation energy jumps from $\Delta E_1 = 0.08$ eV (region I) to $\Delta E_2 = 0.44$ eV (region II). Adopting this model to region I, where in this frequency range the observed time is too short for all jumps (proton) to be successful, the neighbourhood cannot relax to the new position of the proton after it jumps. As a consequence, the activation energy (region II) involved in this translational and/or rotational hopping is much higher than in (region I).

4 Conclusions

Single crystals of $[CAP]_2CuCl_4$ have been grown from an aqueous solution by a slow evaporation technique. This

compound belongs to the monoclinic system with C2/c space group. The structure of this compound consists of (CAP) cations and $[CuCl_4]^{2-}$ anions which are intermediate between tetrahedral and square plane. The structure is stabilized by the N–H···Cl hydrogen bonds (N: pyridine and N: amine) and cation–cation π-lone pair of nitrogen element (N: amine) interactions.

Differential scanning calorimetric and electric measurements were carried out; they showed the evaporation of the water molecules at the temperature range 318–358 K. The activation energy issued from the impedance spectra suggests a protonic conductivity for this material, assigned by the mechanism of hopping.

The number of solid state ^{13}C, ^{63}Cu MAS-NMR components is in full agreement with that of the crystallographically independent site.

5 Supplementary Data

CCDC 755531 contain the supplementary crystallography data for $[CAP]_2CuCl_4$. These data can be obtained free of charge via http://www.ccdc.cam.ac.uk/conts/retrieving.html, or from the Cambridge Crystallographic Data Centre, 12 Union Road, Cambridge CB2 1EZ, UK; fax: (+44) 1223 336 033; or e-mail: deposit@ccdc.cam.ac.uk.

Acknowledgments We would like to thank the staff of the unit of the solid state under the guidance of Professors Guidara-Gargouri for their help in providing their student researcher Abderrazek Oueslati with the measurements of electrical impedance spectroscopy under the direction of Professor Fouazi Hlel.

References

1. D.B. Mitzi, C.A. Field, W.T.A. Harrison, A.M. Guloy, Nature **369**, 467 (1994)
2. P. Day, Philos. Trans. R. Soc. Lond. A **314**, 145 (1985)
3. D.B. Mitzi, S. Wang, C.A. Field, C.A. Chess, A.M. Guloy, Science **267**, 1473 (1995)
4. G.C. Papavassiliou, Prog. Solid State Chem. **25**, 125 (1997)
5. F.M. Woodward, A.S. Albrecht, C.M. Wynn, C.P. Landee, Phys. Rev. B **65**, 144412 (2002)
6. G.C. Papavassiliou, I.B. Koutselas, A. Terzis, M.H. Whangbo, Solid State Commun. **91**, 695 (1994)
7. J.G. Bednorz, K.A. Mueller, Z. Phys. B **64**, 189 (1986)
8. A.J. Millis, I. Shraian, R. Mueller, Phys. Rev. Lett. **77**, 175 (1996)
9. K.E. Halvorson, C. Patterson, R.D. Willett, Acta Crystallogr. B **46**, 508 (1990)
10. P.H. Hammer, D.C. Dender, D.H. Reich, A.S. Albrecht, C.P. Landee, J. Appl. Phys. **81**(8), 4615 (1997)
11. F.C. Coomer, V. Bondah-Jagalu, K.J. Grant, A. Harrison, G.J. Mclntyre, H.M. Ronnow, R. Feyerherm, T. Wand, M. Meibner, D. Visser, D.F. McMorrow, Phys. Rev. B **75**, 094424 (2007)
12. T.J. Coffey, C.P. Landee, W.T. Robinson, M.M. Turnbull, M. Winn, F.M. Woodward, Inorg. Chim. Acta **303**, 54 (2000)
13. A. Weselucha-Birczynska, B. Oleksyn, C. Paluszkiewicz, J. Sliwinski, J. Mol. Struct. **512**, 301 (1999)
14. M. Parvez, A.P. Sabir, Acta Crystallogr. C **53**, 678 (1997)
15. M. Parvez, A.P. Sabir, Acta Crystallogr. C **53**, 679 (1997)
16. G.S. Long, M.Y. Wei, R.D. Willett, Inorg. Chem. **36**, 3102 (1997)
17. V. Fernandez, J.C. Doadrio, S. Garcia-Granda, P. Pertierra, Acta Crystallogr. C **52**, 1412 (1996)
18. Z.M. Wang, R.D. Willett, S. Molnar, K.J. Brewer, Acta Crystallogr. Sect. C **52**, 581 (1996)
19. G. Valle, Acta Crystallogr. C **51**, 2273 (1995)
20. R.D. Willett, Acta Crystallogr. C **51**, 1517 (1995)
21. B. Viossat, N.H. Dung, N. Rodier, Acta Crystallogr. C **51**, 628 (1995)
22. A. Mahoui, J. La Passet, J. More, T.P. Saint Gregoire, Z. Kristallogr. **210**, 125 (1995)
23. C.L. Bouchard, M.A. Hitchman, B.W. Skelton, A.H. White, Aust. J. Chem. **48**, 771 (1995)
24. R.D. Willett, Coord. Chem. Rev. **109**, 181 (1991)
25. D. Massiot, H. Theile, A. Germany, Bruker Rep. **43**, 140 (1994)
26. G.M. Sheldrick, *SHELXS-86, Program for Crystal Structure Solution* (University of Göttingen, Germany, 1986)
27. G.M. Sheldrick, *SHELXL-97, Program for Crystal Structure Refinement* (University of Göttingen, Germany, 1997)
28. L.J. Farrugia, J. Appl. Crystallogr. **30**, 565 (1997)
29. K. Brandenburg, *Diamond Version 2.0* (Impact Gbr, Bonn, Germany, 1998)
30. K.E. Halvorson, C. Patterson, R.D. Willett, Acta Crystallogr. **B46**, 508 (1990)
31. C.A. Hunter, J.K.M. Sanders, J. Am. Chem. Soc. **112**, 5525 (1990)
32. Y.Y. Zheng, G. Wu, M. Deng, H.Z. Chen, M. Wang, B. Zhong Tang, J. Thin Solid Films **127**, 131 (2006)
33. M. Bakiler, I.V. Maslov, S. Akyuz, J. Mol. Struct. **475**, 83–92 (1999)
34. A.K. Rai, R. Singh, K.N. Singh, V.B. Singh, Spectrochim. Acta A. **63**, 483 (2006)
35. A. Marzotto, D.A. Clemente, F. Benetollo, G. Valle, Polyhedron. **20**, 171 (2001)
36. P.L. Goggin, R.J. Goodfellow, K. Kessler, J. Chem Soc. Dalton Trans. 1914 (1977)
37. E. Quiroz-Castro, S. Bernès, N. Barba-Behrens, R. Tapia-Benavides, R. Contreras, He. Nöth, Polyhedron. **1479**, 1484 (2000)
38. K. Chruszcz, M. Barańska, K. Czarniecki, B. Boduszek, L.M. Proniewicz, J. Mol. Struct. **648**, 215–224 (2003)
39. J.R. Macdonald, in *Impedance Spectroscopy*, Chapter 4. (Wiley, New York, 1987)
40. D.C. Sinclair, A.R. West, J. Appl. Phys. **66**, 3850 (1989)
41. F. Yakuphanoglu, Ph.D. Thesis, Firat University, Elazig, Turkey, 2002
42. Y. Aydogdu, F. Yakuphanoglu, A. Aydogdu, M. Sekerci, Y. Balci, I. Aksoy, Synth. Met. **107**, 1991 (1999)
43. Y. Aydogdu, F. Yakuphanoglu, A. Aydogdu, E. Tas, A. Cukurovali, Solid State Sci. **4**, 879 (2002)
44. I. Chaabane, F. Hlel, K. Guidara, Alloys Compd **461**, 495–500 (2008)